On the response bounds of damaged Euler-Bernoulli beams with switching cracks under moving masses

A. Cicirello[a,*]

[a]*Department of Engineering Science, University of Oxford, Parks Road, Oxford OX1 3PJ, UK*

Abstract

The response of damaged Euler-Bernoulli beams with any number of unilateral cracks and subjected to one or more moving masses which remain always in contact with the beam are investigated in this paper. A flexibility switching crack model is employed here to represent a crack as either open or closed at a particular instant depending on the sign of the axial strain at the crack centre and taking into account the location of the crack either at the top or bottom of the beam. This model leads to closed-form solutions of the damaged beam mode shapes as a function of four integration constants, which can be computed by enforcing the boundary conditions, and a Boolean switching crack array which identifies the open cracks. Based on this switching crack model, an efficient computational procedure is proposed to tackle the problems of multiple masses moving on a multi-cracked beam with generic boundary conditions. The proposed procedure is applied to three beams with switching cracks under moving masses, and the results

*Corresponding author
Email address: alice.cicirello@eng.ox.ac.uk (A. Cicirello)

obtained are compared to the widely adopted always open cracks model, showing significant differences. In particular, it is shown that: (i) flexible boundary conditions, multiple switching cracks and multiple moving masses can be easily accounted for with the proposed approach; (ii) the two limiting conditions of always open cracks and always closed cracks (undamaged) models do not always provide bounds on the dynamic response of a beam with switching cracks subject to moving masses; (iii) the side where each crack is located can largely affect the response.
Keywords: Damaged Euler-Bernoulli beams, Moving masses, Discrete spring model, Flexibility crack model, Switching crack model

1. Introduction

The investigation of the response of engineering structures subject to loads which vary in time and space has been the subject of much research attention in the last decades [1, 2]. This is because the transversal displacements and stresses resulting from moving loads can be significantly larger than those obtained in the static loading case. In addition to this, the dynamic performance of a structure can be largely affected by the presence of damages. This problem is particularly relevant when dealing with bridges subject to moving vehicles, where cracks, local material deterioration and structural joint damages caused by environmental and loading conditions can lead to excessive deflections or unexpected bridge failures [2].

In this work, the moving load-bridge interaction problem is treated by using the well-established model of an Euler-Bernoulli beam subject to moving masses. With this model both force and inertia effects of the moving load

are taken into account producing time-varying mass, stiffness and damping matrices, however the elastic and damping properties of the moving object are disregarded [1, 2]. This model provides very often a good compromise in terms of computational cost and solution accuracy compared to more complex models, such as those considering a structure subject to a sprung mass model or detailed Finite Element models of the two interacting elements [2]. When dealing with global performance of structures, the presence of damage is often tackled by using a discrete spring model [3]. This model provides the best trade-off between model accuracy and computational cost compared to local stiffness reduction models and to 2D/3D Finite Element models which include crack initiation and propagation [3, 4].

The discrete spring crack model was applied to the analysis of a damaged undamped Euler-Bernoulli beam subject to a moving mass by Bilello and Bergman in reference [5]. In particular, they used a massless rotational spring to represent each crack, and the governing equations were written for each undamaged pieces between two consecutive cracks. With this formulation, the size of the problem increases with the number of cracks, since a set of continuity conditions need to be imposed at each crack location. Pala and Reis [6] recently investigated the problem of a simply supported beam with one open crack subject to a moving mass using a different approach. Specifically, they modelled the crack using the flexibility model developed by Chondros et al. [7] and approximated the solution of the governing differential equations considering separately the conditions when the load is moving over the crack or over the undamaged beam section.

The open crack model can lead to inaccurate results in the presence of

capillary cracks, which can open and closed depending on the vibration amplitude and side where the damage is located (i.e. either top or bottom fibres). This can be accounted for by employing the switching crack model or the breathing cracks model. While the former accounts for the closed crack condition and the residual cross section stiffness when the crack is open, the latter accounts for progressive variations of the cross section stiffness. Nonetheless, very few studies have addressed the effects of switching or breathing cracks for moving load problems.

Recently, Ariaei et al. [8] have investigated the dynamic response of a beam with a breathing crack under a moving mass. In particular, they have used the so-called Discrete Element Technique (DET) which substitute the continuous beam with an assembly of rigid elements and flexible joints. This approach was applied to a simply supported beam under a moving mass and their results were benchmarked with a Finite Element model. However, as discussed by the authors, the DET formulation can become very complicated, and it is affected by discretization and round-off errors. In their paper it was concluded that a simply supported beam with a breathing crack subject to a moving mass displayed lower deflection compared to a beam with an open crack. The same conclusion was obtained by Nguyen et al. [9]. Fu [10] has recently tackled the problem of a simply-supported beam with multiple switching cracks by using the local stiffness reduction model and considering moving vehicles modelled as a sprung-mass system. This contribution has shown that 2 and 4 switching cracks can lead to a larger displacements than open cracks, and that the beam response is influenced by the velocity of the vehicles, which in turn can increase the contribution of particular modes

(being the velocity of the vehicle closer to one of the beam natural frequency). The method developed by Fu [10] considers that all the cracks are on the bottom side of the beam, which might not always be the case, and yields the mode shapes of the cracked beam by using a matrix iterative approach, which can require a large computational cost.

The objective of the present work is to present an approach for efficiently assessing the response of Euler-Bernoulli beams with multiple switching cracks and generic boundary conditions when subject to one or more moving masses. This enables to investigate if the response obtained with the always open or always closed (undamaged) models can provide bounds on the response obtained with the switching crack models. This approach is based on: (i) extending the recently developed flexibility model of switching cracks [11] to transient analysis, by providing a closed-form expression of the mode shapes of a cracked beam with any number of cracks that can be at the top and bottom of the beam; (ii) employing an efficient numerical integration scheme based on the transition matrix for treating the always-open crack case; (iii) decomposing the switching crack problem as a sequence of linear transient analysis by identifying the so-called "transition instants".

The paper is organised as follows: the governing equations of the damaged beam under moving masses are derived in Section 2. The flexibility model of switching cracks is extended to dynamics problems in Section 3 and applied to yield a closed-form expression of the mode shapes of an Euler-Bernoulli beam with multiple cracks. A computational strategy for the transient analysis of Euler-Bernoulli beams with multiple switching cracks and generic boundary conditions subject to moving masses is presented in Section 4 and validated

in Section 5.

2. Damaged beam under moving masses: governing equations

Let us consider a vehicle travelling with a constant speed on a damaged bridge. The vehicle can be modelled as a mass with a constant pre-load which correspond to its own weight, and the bridge can be modelled as an Euler-Bernoulli damaged beam [2]. In the following developments, the general case of an inhomogeneous beam will be considered at first, and then the problem will be particularised by using the flexibility model of switching cracks.

The beam-moving mass interaction can be investigated by making the following common assumptions [2]: i) given the relative small size of the interaction problem, the friction force is neglected; ii) the mass is travelling with known direction and speed along the z-axis; iii) the vibration of the beam occurs only in the transversal direction; iv) the mass and the beam are always in contact. Given these assumptions, the equation governing the transverse motion $u(z,t)$ (positive if downward) of an inhomogeneous undamped beam subject to a moving mass (m) with constant speed v can be written as [12]:

$$\frac{\partial^2}{\partial z^2}\left[E(z)I(z)\frac{\partial^2 u(z,t)}{\partial z^2}\right]+\mu\frac{\partial^2 u(z,t)}{\partial t^2}=F(z,t). \tag{1}$$

where t is the time variable, z is the spatial coordinate spanning from 0 to the length L of the member, $E(z)I(z)$ is the abscissa-dependent flexural stiffness being $E(z)$ and $I(z)$ are the Young's modulus and second moment of area, respectively, and μ is the mass per unit length of the beam. The loading

$F(z,t)$ is given by [12]:

$$F(z,t) = m(\mathrm{g} - a_t)\delta(z - vt). \tag{2}$$

where the Dirac delta function $\delta(z - vt)$ accounts for the position of the mass on the beam and therefore it specifies the excitation point, $m\,\mathrm{g}$ is a constant force corresponding to the weight of the moving mass (where m is the mass and g is the gravitational acceleration), $m\,a_t$ is a dynamic force due to the moving mass where a_t is the transverse acceleration of the moving mass which is given by:

$$a_t = \left(\frac{\partial^2}{\partial t^2} u(z,t) + 2v \frac{\partial^2}{\partial z \partial t} u(z,t) + v^2 \frac{\partial^2}{\partial z^2} u(z,t) \right). \tag{3}$$

The first term on the r.h.s. of Eq. (3) is the vertical component of the acceleration, the second term is the Coriolis acceleration and the last term corresponds to the centripetal acceleration of the moving mass.

The solution of Eq. (1) is commonly obtained by using the mode superposition method [2, 12], which expand the deflection of the beam as a linear combination of time-dependent modal amplitudes and spatially-dependent mode shapes. In particular, the undamped inhomogeneous beam mode shapes are considered, ignoring the presence of the moving object, since the mass of the moving object is usually much lower than that of the beam. If the moving object mass effect has to be taken into account, this would result into time-varying mode shapes which depend on the mass position, therefore not allowing the application of the mode superposition method. In this paper, the effect of the moving mass on the beam mode shapes is assumed negligible.

Let us now consider the case of a damaged beam with cracks specified by the vector $\mathbf{\Lambda}$ with entries λ_j equal to 1 if the jth crack is open, or 0 if the jth

crack is closed (no crack), so that the transversal deflection is indicated with $u(z,t,\mathbf{\Lambda})$. The mode superposition method can be applied by considering the mode shapes of a damaged beam [13, 14], so that:

$$u(z,t,\mathbf{\Lambda}) = \sum_{r=1}^{\infty} \phi_r(z,\mathbf{\Lambda}) q_r(t) \tag{4}$$

where $\phi_r(z,\mathbf{\Lambda})$ is the r-th mode shape of a damaged beam with open cracks specified by the vector $\mathbf{\Lambda}$, and $q_r(t)$ is the r-th generalised coordinate. A modal truncation is often performed, so that:

$$u(z,t,\mathbf{\Lambda}) \cong \sum_{r=1}^{N} \phi_r(z,\mathbf{\Lambda}) q_r(t) \tag{5}$$

where N is the number of modes which are included in the modal expansion. Considering a sufficient number of modes would produce a small error in the response calculation. As a rule-of-thumb, N can be chosen as twice the number of modes that would be excited by the load acting on the beam.

A dimensionless abscissa $\zeta = z/L$ which takes values from 0 to 1 is introduced, so that the mode shapes can be written in dimensionless form:

$$\widetilde{\phi}(\zeta) = \frac{\phi(\zeta\, L)}{L}; \tag{6}$$

By using this dimensionless form, and substituting Eq. (5) into Eq. (1), the following expression is obtained:

$$\sum_{r=1}^{N} \left[E(\zeta L) I(\zeta L)\, \widetilde{\phi}_r{}''(\zeta,\mathbf{\Lambda}) q_r(t) \right]'' + \mu \sum_{r=1}^{N} \widetilde{\phi}_r(\zeta,\mathbf{\Lambda}) \ddot{q}_r(t) = F(\zeta L, t) \tag{7}$$

where the prime denotes differentiation with respect to the dimensionless abscissa ζ, the dot denotes differentiation with respect to time . The loading

term can be written as:

$$F(\zeta L,t)=m\Big[\mathrm{g}-\sum_{r=1}^{N}\widetilde{\phi}_r(\zeta,\mathbf{\Lambda})\ddot{q}_r(t) - \widetilde{v}^2\sum_{r=1}^{N}\widetilde{\phi}_r''(\zeta,\mathbf{\Lambda})q_r(t)-2\widetilde{v}\sum_{r=1}^{N}\widetilde{\phi}_r'(\zeta z,\mathbf{\Lambda})\dot{q}_r(t)\Big]\delta(\zeta-\widetilde{v}t) \quad (8)$$

where $\widetilde{v}=v/L$. Multiplying each term of Eq. (7) by $\widetilde{\phi}_s(\zeta,\mathbf{\Lambda})$ and integrating along the (dimensionless) length of the beam yield:

$$\sum_{r=1}^{N}\int_0^1\widetilde{\phi}_s(\zeta,\mathbf{\Lambda})\left[E(\zeta L)I(\zeta L)\,\widetilde{\phi}_r{}''(\zeta,\mathbf{\Lambda})\right]''q_r(t)\mathrm{d}\zeta + \mu\sum_{r=1}^{N}\int_0^1\widetilde{\phi}_r(\zeta,\mathbf{\Lambda})\widetilde{\phi}_s(\zeta,\mathbf{\Lambda})\ddot{q}_r(t)\mathrm{d}\zeta=\int_0^1\widetilde{\phi}_s(\zeta,\mathbf{\Lambda})F(\zeta L,t)\mathrm{d}\zeta \quad (9)$$

The mode shape between two successive cracks can be described as that of the undamaged beam. Therefore, the mode shape of a damaged beam can be considered as a superposition of the mode shapes of undamaged beams. Consequently, the orthogonality properties of the damaged beam mode shapes with respect to the mass and the stiffness hold [13, 14], so that:

$$\mu\int_0^1\widetilde{\phi}_r(\zeta,\mathbf{\Lambda})\widetilde{\phi}_s(\zeta,\mathbf{\Lambda})\mathrm{d}\zeta=M_r\delta_{rs} \quad (10)$$

$$\int_0^1\widetilde{\phi}_s(\zeta,\mathbf{\Lambda})\left[E(\zeta L)I(\zeta L)\,\widetilde{\phi}_r{}''(\zeta,\mathbf{\Lambda})\right]''\mathrm{d}\zeta=K_r\delta_{rs} \quad (11)$$

where δ_{rs} is the Kronecker delta which is defined as:

$$\delta_{rs}=\begin{cases}0, & \text{if r}\neq\text{s}\\ 1, & \text{if r}=\text{s}\end{cases}. \quad (12)$$

and M_r and K_r are, respectively, the modal mass and modal stiffness of the r-th damaged beam mode. These matrices are related via:

$$K_r=\omega_r^2M_r \quad (13)$$

being ω_r the r-th natural frequency of the beam. By using these relations (Eq. (10), Eq. (11) and Eq. (13)) and after some algebraic manipulations of Eq. (9), the following equation is obtained for the r-th mode:

$$\ddot{q}_r(t) + \omega_r^2 q_r(t) = \frac{1}{M_r} \int_0^1 \widetilde{\phi}_s(\zeta, \mathbf{\Lambda}) F(\zeta L, t) \mathrm{d}\zeta \tag{14}$$

For $r = 1, ...N$, Eq. (14) represents a set of r coupled second order differential equations. These equations can be written in a dimensionless and more compact form. Specifically, the right hand side of Eq. (14) can be obtained by using Eq. (8). The resulting integrals can be easily evaluated by using the Dirac delta properties, leading to the following expression: :

$$\begin{aligned} \frac{1}{M_r} \int_0^1 \widetilde{\phi}_s(\zeta, \mathbf{\Lambda}) \widetilde{F}(\zeta, t) \mathrm{d}\zeta = \frac{L^2}{EI_0} \frac{m}{M_r} \widetilde{\phi}_s(\widetilde{v}t, \mathbf{\Lambda}) \Big[\mathrm{g} - \sum_{r=1}^{N} \widetilde{\phi}_r(\widetilde{v}t, \mathbf{\Lambda}) \ddot{q}_r(t) \\ - \widetilde{v}^2 \sum_{r=1}^{N} \widetilde{\phi}_r''(\widetilde{v}t, \mathbf{\Lambda}) q_r(t) - 2\widetilde{v} \sum_{r=1}^{N} \widetilde{\phi}_r'(\widetilde{v}t, \mathbf{\Lambda}) \dot{q}_r(t) \Big]. \end{aligned} \tag{15}$$

where $\widetilde{F}(\zeta, t) = (F(\zeta L, t) L^2)/(EI_0)$. By substituting Eq. (15) into Eq. (14) and re-arranging the terms, the governing equations of motion can be written as:

$$\hat{\mathbf{M}}(t)\ddot{\mathbf{q}}(t) + \hat{\mathbf{D}}(t)\dot{\mathbf{q}}(t) + \hat{\mathbf{K}}(t)\mathbf{q}(t) = \hat{\mathbf{F}}(t), \tag{16}$$

where $\mathbf{q}(t)$ is a N-dimensional array collecting the $q_r(t)$, while the modal mass ($\hat{\mathbf{M}}(t)$), damping ($\hat{\mathbf{D}}(t)$) and stiffness ($\hat{\mathbf{K}}(t)$) matrices are given by a constant term, arising from the beam, plus a time-varying term, due to the moving mass, such that:

$$\hat{\mathbf{M}}(t) = \bar{\mathbf{M}} + \Delta\mathbf{M}(t)\,; \tag{17}$$

$$\hat{\mathbf{D}}(t) = \bar{\mathbf{D}} + \Delta\mathbf{D}(t)\,; \tag{18}$$

$$\hat{\mathbf{K}}(t) = \bar{\mathbf{K}} + \Delta\mathbf{K}(t)\,. \tag{19}$$

It can be easily shown that each entry of $\hat{\mathbf{M}}(t)$, $\hat{\mathbf{D}}(t)$ and $\hat{\mathbf{K}}(t)$ matrices is given by:

$$[\hat{\mathbf{M}}(t)]_{rs} = \delta_{rs} + \frac{L^2}{EI_0}\frac{m}{M_r}\widetilde{\phi}_r(\widetilde{v}t, \mathbf{\Lambda})\widetilde{\phi}_s(\widetilde{v}t, \mathbf{\Lambda}); \tag{20}$$

$$[\hat{\mathbf{D}}(t)]_{rs} = 0 + \frac{L^2}{EI_0}\frac{2\widetilde{v}m}{M_r}\widetilde{\phi}_r(\widetilde{v}t, \mathbf{\Lambda})\widetilde{\phi}'_s(\widetilde{v}t, \mathbf{\Lambda}); \tag{21}$$

$$[\hat{\mathbf{K}}(t)]_{rs} = \omega_r^2\delta_{rs} + \frac{L^2}{EI_0}\frac{\widetilde{v}^2m}{M_r}\widetilde{\phi}_r(\widetilde{v}t, \mathbf{\Lambda})\widetilde{\phi}''_s(\widetilde{v}t, \mathbf{\Lambda}); \tag{22}$$

and each entry of the time-varying force vector $\hat{\mathbf{F}}(t)$ is given by:

$$[\hat{\mathbf{F}}(t)]_r = \frac{L^2}{EI_0}\frac{mg}{M_r}\widetilde{\phi}_r(\widetilde{v}t, \mathbf{\Lambda}). \tag{23}$$

Eq. (16) represents a set of N-coupled second-order differential equations of motion with time-varying inertia, damping and stiffness. The equation of motion of the r-th mode is given by:

$$\begin{aligned}\Big[1 + \frac{L^2}{EI_0}\frac{m}{M_r}\widetilde{\phi}_r(\widetilde{v}t, \mathbf{\Lambda})\widetilde{\phi}_r(\widetilde{v}t, \mathbf{\Lambda})\Big]\ddot{q}_r(t) + \frac{L^2}{EI_0}\frac{2\widetilde{v}m}{M_r}\widetilde{\phi}_r(\widetilde{v}t, \mathbf{\Lambda})\widetilde{\phi}'_r(\widetilde{v}t, \mathbf{\Lambda})\dot{q}_r(t) \\ + \Big[\omega_r^2 + \frac{L^2}{EI_0}\frac{\widetilde{v}^2m}{M_r}\widetilde{\phi}_r(\widetilde{v}t, \mathbf{\Lambda})\widetilde{\phi}''_r(\widetilde{v}t, \mathbf{\Lambda})\Big]q_r(t) = \frac{L^2}{EI_0}\frac{mg}{M_r}\widetilde{\phi}_r(\widetilde{v}t, \Lambda).\end{aligned} \tag{24}$$

It is worth noting that when $[\hat{\mathbf{M}}(t)]_{rs} = \delta_{rs}$, $[\hat{\mathbf{D}}(t)]_{rs} = 0$ and $[\hat{\mathbf{K}}(t)]_{rs} = \omega_r^2\delta_{rs}$, and $\mathbf{\Lambda} = \mathbf{0}$, the governing equation of an undamaged beam under a moving force is recovered [15]. While if $\mathbf{\Lambda} = \mathbf{1}$, then the governing equation of a multi-cracked beam under a moving force is recovered [13]. The solution of this problem has been addressed by Caddemi et al. [13] exploiting the rigidity crack model [14] and accounting for switching cracks, but not the effect of moving masses.

The problem can be generalised by considering the effects of p moving masses each with constant velocity v_j starting from the abscissa ζ_{m_j}, being

$j = 1...p$. The mass that takes longer to get to the end of the beam is mass 1, and this mass defines the duration of the transient analysis $t_f = (l - \zeta_{m_1})/v_1$. In this case, Eq. (20), Eq. (21), Eq. (22) and Eq. (23) can be generalised to:

$$[\hat{\mathbf{M}}(t)]_{rs} = \delta_{rs} + \frac{L^2}{EI_0}\sum_{j=1}^{p}\frac{m_j}{M_r}\widetilde{\phi}_r(\zeta_{m_j} + \widetilde{v}_j t, \mathbf{\Lambda})\widetilde{\phi}_s(\zeta_{m_j} + \widetilde{v}_j t, \mathbf{\Lambda})\mathrm{U}[1 - (\zeta_{m_j} + \widetilde{v}_j t)]; \tag{25}$$

$$[\hat{\mathbf{D}}(t)]_{rs} = 0 + \frac{L^2}{EI_0}\sum_{j=1}^{p}\frac{2\widetilde{v}_j m_j}{M_r}\widetilde{\phi}_r(\zeta_{m_j} + \widetilde{v}_j t, \mathbf{\Lambda})\widetilde{\phi}'_s(\zeta_{m_j} + \widetilde{v}_j t, \mathbf{\Lambda})\mathrm{U}[1 - (\zeta_{m_j} + \widetilde{v}_j t)]; \tag{26}$$

$$[\hat{\mathbf{K}}(t)]_{rs} = \omega_r^2\delta_{rs} + \frac{L^2}{EI_0}\sum_{j=1}^{p}\frac{\widetilde{v}_j^2 m_j}{M_r}\widetilde{\phi}_r(\zeta_{m_j} + \widetilde{v}_j t, \mathbf{\Lambda})\widetilde{\phi}''_s(\zeta_{m_j} + \widetilde{v}_j t, \mathbf{\Lambda})\mathrm{U}[1 - (\zeta_{m_j} + \widetilde{v}_j t)]; \tag{27}$$

$$[\hat{\mathbf{F}}(t)]_r = \frac{L^2}{EI_0}\sum_{j=1}^{p}\frac{m_j \mathrm{g}}{M_r}\widetilde{\phi}_r(\zeta_{m_j} + \widetilde{v}_j t, \mathbf{\Lambda})\mathrm{U}[1 - (\zeta_{m_j} + \widetilde{v}_j t)]; \tag{28}$$

where $\mathrm{U}[1 - (\zeta_{m_j} + \widetilde{v}_j t)]$ is the Unit Step function that switches off the contribution of the moving masses that reach the end of the beam. Specifically, $\mathrm{U}[1 - (\zeta_{m_j} + \widetilde{v}_j t)]$ is equal to 1 when $(\zeta_{m_j} + \widetilde{v}_j t) \leq 1$, zero otherwise.

The solution of Eq. (16) yields the vector $\mathbf{q}(t)$. This is then substituted into Eq. (5) to yield the transient response of a damaged beam with multiple open cracks subject to moving masses. Efficient computational strategies for establishing the solution of Eq. (16) under multiple switching cracks are developed by using the closed-form the expression of the mode shapes of a damaged beam, as discussed in the next sections.

3. Damaged Euler-Bernoulli beam mode shapes using the flexibility model of switching cracks

3.1. Extension of the flexibility model of switching crack to a transversally vibrating damaged beam

The flexibility model of switching cracks [11] considers a crack as open or closed depending on the sign of elastic axial strain calculated at the crack centre and the side where the crack is located. This model is based on some common macro-scale assumptions on the behaviour of cracks, that is: *i*) when cracks are open, they can be modelled through equivalent internal springs with a linear moment-rotation constitutive law; and *ii*) degradation effects are negligible, that is the cracks depth remains constant. These assumptions are valid if the loadings acting on the structural member are below threshold values that may cause the cracks to open further.

With this model, the dimensionless bending flexibility of the beam

$$\widetilde{EI}(\zeta) = \frac{E(\zeta\, L)\, I(\zeta\, L)}{EI_0}\,, \tag{29}$$

where the over-tilde denotes the dimensionless function of ζ and EI_0 is a convenient reference value of the flexural stiffness, is given by [11]:

$$\widetilde{EI}(\zeta)^{-1} = 1 + \sum_{j=1}^{n} \alpha_j\, \lambda_j\, \delta(\zeta - \bar{\zeta}_j)\,. \tag{30}$$

where n is the number of cracks, the jth one occurring at the dimensionless abscissa $\bar{\zeta}_j = \bar{z}_j/L$; $\delta(\zeta - \bar{\zeta}_j)$ is the Dirac delta function centred at the jth crack position; λ_j is the so-called switching crack variable that is a Boolean variable which take the values of 1 if a crack is open or 0 when the crack is

closed; α_j is a dimensionless parameter related to the severity of the damage at $\zeta = \bar{\zeta}_j$ and is given by:

$$\alpha_j = \frac{EI_0}{K_j\, L} = \frac{1}{\widetilde{K}_j}\,, \tag{31}$$

where K_j is the elastic stiffness of the rotational spring and $\widetilde{K}_j$ is its dimensionless counterpart.

The transition from open to closed in the static analysis of damaged Euler-Bernoulli beam-column is expressed as [11]:

$$\lambda_j = \begin{cases} 0, & \widetilde{\epsilon}_j \leq 0 \\ 1, & \widetilde{\epsilon}_j > 0 \end{cases} \tag{32}$$

where $\widetilde{\epsilon}_j$ is the elastic axial strain at the jth crack (positive if the fibre at the centre of the crack is stretching; negative if compressing), which is given by:

$$\widetilde{\epsilon}_j = \frac{\mathscr{N}(\bar{\zeta}_j\, L)}{EA_0} + \frac{\mathscr{M}(\bar{\zeta}_j\, L)}{EI_0}\bar{y}_j \tag{33}$$

where $\mathscr{N}(\bar{\zeta}_j\, L)$ is the axial force at $z = \bar{z}_j$ (which is positive in tension and negative in compression); EA_0 is the axial rigidity (where A_0 is the undamaged cross-sectional area); $\mathscr{M}(\bar{\zeta}_j\, L)$ is the bending moment about the neutral axis; $\bar{y}_j$ is the distance between neutral axis and jth crack centre: when $\bar{y}_j > 0$, the jth crack occurs on the bottom side of the beam and it tends to open when the beam is sagging, while the opposite happens when $\bar{y}_j < 0$. When all the λ_j parameters are set to 1, the flexibility model of switching crack [11] reduces to the flexibility model of cracks [16] which considers always open cracks.

In a moving mass problem, the transversal vibration of each point of the beam will vary depending on the mass position and speed. As a result, at

a given time instant, the induced deformation might lead to the opening of some cracks, and closing of some others. The dynamic response of the damaged beam can be modelled as a sequence of time intervals in which the crack distribution remains unchanged [10, 13]. Therefore, the flexibility model of switching cracks can be easily extended to the transient analysis by evaluating a transition instant which is characterised by a new crack distribution. In particular, at each time step T_s of the dynamic analysis, the open cracks distribution of a transversally vibrating damaged beam has to be assessed by calculating at each crack location, $\bar{\zeta}_j = z_j/l$, the axial strain. In the absence of axial loading, the axial strain can be written as:

$$\widetilde{\epsilon}_j(t_s) = \frac{\mathscr{M}(\bar{\zeta}_j\, L, t_s)}{EI_0}\bar{y}_j \tag{34}$$

where $\mathscr{M}(\bar{\zeta}_j\, L, T_s)$ is the bending moment at the crack location at the time step t_s ($\mathscr{M}(\bar{\zeta}_j\, L, T_s) = -EI(z_j)u''(z_j, T_s) = -EI(z_j)\sum_{r=1}^{N}\phi_r''(\bar{\zeta}_j\, L, \mathbf{\Lambda})q_r(T_s)$).

The time dependent switching cracks parameters $\lambda_j(T_s)$ can be therefore obtained as:

$$\lambda_j(T_s) = \begin{cases} 0, & \widetilde{\epsilon}_j(T_s) \leq 0 \\ 1, & \widetilde{\epsilon}_j(T_s) > 0 \end{cases} \tag{35}$$

These $\lambda_j(T_s)$ are then collected in the array $\mathbf{\Lambda}_{T_s} = \{\lambda_1(T_s), \cdots, \lambda_n(T_s)\}$.

Since the dynamic response of the damaged beam can be considered as a sequence of time intervals in which the crack distribution is specified by $\mathbf{\Lambda}_{T_s}$, it is possible to derive the analytical expressions of the damaged beam mode shapes as a function of four integration constants (to be computed by enforcing the boundary conditions) and a general Boolean switching crack array $\mathbf{\Lambda}$ which identifies the open cracks.

3.2. Natural frequencies and mode shapes of Euler-Bernoulli beams with multiple cracks

The closed-form solution for the mode shapes of a slender beam with multiple cracks $\mathbf{\Lambda}$ can be derived by means of the Laplace transform and its inverse. Starting from this solution, the corresponding natural frequencies can be also obtained.

The differential equation which governs the free vibration of an inhomogeneous beam transverse vibration is obtained by setting $F(\zeta L, t) = 0$ in Eq. (7), so that:

$$\sum_{r=1}^{N} \left[E(\zeta L) I(\zeta L) \, \widetilde{\phi}_r{}''(\zeta, \mathbf{\Lambda}) q_r(t) \right]'' + \mu \sum_{r=1}^{N} \widetilde{\phi}_r(\zeta, \mathbf{\Lambda}) \ddot{q}_r(t) = 0 \tag{36}$$

After simple manipulations, this equation can be rewritten for each r-mode as:

$$\frac{\left[E(\zeta L) I(\zeta L) \, \widetilde{\phi}_r{}''(\zeta, \mathbf{\Lambda}) \right]''}{\mu \widetilde{\phi}_r(\zeta, \mathbf{\Lambda})} = -\frac{\ddot{q}_r(t)}{q_r(t)} \tag{37}$$

Since the left hand side of this equation is a function of ζ only, while the right hand side is a function of t only, both members must be equal to a constant ω_r^2. Therefore, two differential equations are obtained:

$$\ddot{q}_r(t) + \omega_r^2 q_r(t) = 0 \tag{38}$$

whose solution is harmonic, and

$$\left[E(\zeta L) I(\zeta L) \, \widetilde{\phi}_r{}''(\zeta, \mathbf{\Lambda}) \right]'' - \omega_r^2 \mu \widetilde{\phi}_r(\zeta, \mathbf{\Lambda}) = 0 \tag{39}$$

This can be conveniently rewritten in terms of the flexibility model of crack (Eq. (29) and Eq. (30)) and in dimensionless form, so that:

$$\left[\widetilde{EI}(\zeta) \widetilde{\phi}_r''(\zeta) \right]'' - \beta_r^4 \widetilde{\phi}_r(\zeta) = 0; \tag{40}$$

where:

$$\beta_r^4 = \frac{\mu\, L^4\, \omega_r^2}{EI_0}. \tag{41}$$

The solution of Eq. (40) yields a closed-form expression for the r-th mode shape of a multi-cracked beam. In order to simplify the notation, the subscript r is omitted in what follows. Initially Eq. (40) is integrated twice, to yield:

$$\left[\widetilde{EI}(\zeta)\widetilde{\phi}''(\zeta)\right] - \beta^4 \widetilde{\phi}^{[2]}(\zeta) = C_A\zeta + C_B\,, \tag{42}$$

where C_A and C_B are two unknown integration constants, while $\widetilde{\phi}^{[m]}(\zeta)$ stands for the primitive (or anti-derivative) of order m of $\widetilde{\phi}(\zeta)$ given by m consecutive indefinite integrations. By setting:

$$\widetilde{W}(\zeta) = \beta^4 \widetilde{\phi}^{[2]}(\zeta) - C_A\zeta - C_B\,, \tag{43}$$

after some algebraic manipulation, Eq. (42) can be then rewritten as:

$$\left[\widetilde{EI}(\zeta)\widetilde{W}''''(\zeta)\right] - \beta^4 \widetilde{W}(\zeta) = 0\,, \tag{44}$$

whose solution can be readily obtained by applying the Laplace transform and its inverse. By taking the second derivative of this solution, the closed-form expression of the mode shape of a damaged beam with specified open cracks is obtained. This can be expressed in compact form as:

$$\begin{aligned}\widetilde{\phi}(\zeta, \mathbf{\Lambda}) &= \gamma''(\zeta) \\ &+ \frac{\beta^3}{2}\sum_{j=1}^{n} \alpha_j \lambda_j \psi_j \left[\sinh\left(\beta\left(\zeta - \bar{\zeta}_j\right)\right) + \sin\left(\beta\left(\zeta - \bar{\zeta}_j\right)\right)\right] H(\zeta - \bar{\zeta}_j)\end{aligned} \tag{45}$$

where:

$$\begin{aligned}\gamma(\zeta) = \frac{1}{2\beta^3}\Big[&\beta(C_1\beta^2 - C_3)\cos(\beta\,\zeta) + \beta(C_1\beta^2 + C_3)\cosh(\beta\,\zeta) \\ &+ (C_2\beta^2 - C_4)\sin(\beta\,\zeta) + (C_2\beta^2 + C_4)\sinh(\beta\,\zeta)\Big]\,,\end{aligned} \tag{46}$$

and:

$$\psi_j = \gamma\left(\bar{\zeta}_j\right) + \frac{\beta}{2}\sum_{k=1}^{j-1}\alpha_k\lambda_k\,\psi_k\left[\sinh\left(\beta\left(\bar{\zeta}_j-\bar{\zeta}_k\right)\right)-\sin\left(\beta\left(\bar{\zeta}_j-\bar{\zeta}_k\right)\right)\right]H(\bar{\zeta}_j-\bar{\zeta}_k)\,, \quad (47)$$

in which $H(\zeta)$ denotes the Heaviside unit step function (which corresponds to the primitive of the Dirac delta function centred at zero):

$$H(\zeta) = \delta^{[1]}(\zeta) = \int_{-\infty}^{\zeta}\delta(\xi)\,\mathrm{d}\xi = \begin{cases} 0, & \zeta < 0\,; \\ \frac{1}{2}, & \zeta = 0\,; \\ 1, & \zeta > 0\,. \end{cases} \quad (48)$$

Eq. (45) represents a superposition of undamaged mode shapes between two successive cracks, therefore satisfying Eq. (10), Eq. (11) and Eq. (13). In particular, when $\mathbf{\Lambda} = \mathbf{1}$, and correspondingly $\widetilde{\phi}(\zeta, \mathbf{1})$, the mode shape expression of a beam with always open cracks is obtained. These equations yield equivalent results to those obtained by Caddemi et al. [14] in which the rigidity crack model was used. For $\mathbf{\Lambda} = \mathbf{0}$, the well-known mode shape expression of the undamaged beam is recovered:

$$\widetilde{\phi}(\zeta,\mathbf{0}) = \gamma''(\zeta) = \frac{1}{2\beta}\Big[\beta(C_3 - C_1\beta^2)\cos(\beta\,\zeta) + \beta(C_1\beta^2 + C_3)\cosh(\beta\,\zeta) + (C_4 - C_2\beta^2)\sin(\beta\,\zeta) + (C_2\beta^2 + C_4)\sinh(\beta\,\zeta)\Big]\,. \quad (49)$$

By enforcing the pertinent boundary conditions in terms of the mode shapes $\widetilde{\phi}(\zeta, \mathbf{\Lambda})$ and its derivatives, the corresponding four integration constants (C_1, C_2, C_3 and C_4) are obtained. Examples of common boundary conditions are given in the Appendix. Each natural frequency of the multi-cracked beam is then obtained in terms of the parameter β (they are related

through Eq. (41)), which is in turn computed as the non-trivial root of the "characteristic equation" that is obtained by setting equal to zero the determinant of the system of the four homogeneous linear equations associated with the boundary conditions. At each natural frequency ω_r, the corresponding mode shape of the damaged beam $\widetilde{\phi}(\zeta, \mathbf{\Lambda})$ is therefore obtained.

4. Dynamic response of a beam with multiple switching cracks under moving masses

In this section two computational strategies are presented to tackle the dynamic response of a beam with always open cracks under moving masses (subsection 4.1), and the dynamic response of a beam with switching cracks under moving masses (subsection 4.2).

4.1. Euler-Bernoulli beam with a set of pre-assigned always open cracks under moving masses

The cracks can be considered as always open and described by $\mathbf{\Lambda}$ when during the passage of the moving masses on the beam, the open crack distribution is not changing. In this case, Eq. (16) can be solved by using the unconditionally stable Newmark integration scheme. Alternatively, it can be solved by re-writing the problem in the state-space form and by using an unconditionally stable step-by-step numerical scheme based on the use of the transition matrix [17, 18]. The latter will be used in what follows.

The second order system of equations Eq. (16) can be rewritten as a set of first order differential equations by using the state-space form of Eq. (16):

$$\dot{\mathbf{y}}(t) = \mathbf{A}(t)\mathbf{y}(t) + \mathbf{V}(t)\hat{\mathbf{F}}(t), \tag{50}$$

where:

$$\mathbf{y}(t) = \begin{bmatrix} \mathbf{q}(t) \\ \dot{\mathbf{q}}(t) \end{bmatrix}; \tag{51}$$

$$\mathbf{A}(t) = \begin{bmatrix} \mathbf{0} & \mathbf{I} \\ -\hat{\mathbf{M}}^{-1}(t)\hat{\mathbf{K}}(t) & -\hat{\mathbf{M}}^{-1}\hat{\mathbf{D}}(t) \end{bmatrix}; \tag{52}$$

and

$$\mathbf{V}(t) = \begin{bmatrix} 0 \\ \hat{\mathbf{M}}^{-1}(t) \end{bmatrix}; \tag{53}$$

The non-homogeneous time-varying set of equations (Eq. (50)) can be solved in an analogous way to the constant-matrix case (see for example reference [17]). This can be achieved by assuming that the time-varying coefficients are constant over each time interval Δt. This condition is obtained by subdividing the time variable in a sufficient number of small intervals of equal length [17, 18]. As a rule-of-thumb, Δt is chosen to be the inverse of 6-10 times the highest modal frequency considered [17]. Under this assumption, an unconditionally stable step-by-step numerical integration scheme can be employed. This approach is based on the evaluation of the so-called transition matrix which is defined as [17, 18]

$$\mathbf{\Theta}\left(\Delta t_k\right) \cong \exp\left[\mathbf{A}(T_k)\Delta t_k\right] \tag{54}$$

where $\Delta t_k = T_{k+1} - T_k$, and $T_k = k\Delta t$ (with $k = 0, 1, ...Y$, being Y the number of Δt considered). The incremental solution is then expressed as:

$$\mathbf{y}(T_{k+1}) = \mathbf{\Theta}\left(\Delta t_k\right)\mathbf{y}(T_k) + \Psi_0\left(\Delta t_k\right)\mathbf{V}(T_k)\hat{\mathbf{F}}(T_k) \tag{55}$$

where

$$\Psi_0\left(\Delta t_k\right) = \left[\mathbf{\Theta}\left(\Delta t_k\right) - \mathbf{I}\right]\mathbf{A}^{-1}(T_k) \tag{56}$$

4.2. Euler-Bernoulli beam with switching cracks subject to moving masses

Let us now consider the flexural vibration of a damaged Euler-Bernoulli beam with n switching cracks subject to moving masses from time $t = 0$ to $T_Y = Y\Delta t$. Because of the effect of the moving masses, the damaged beam will start vibrating transversally and the induced deformed shape at each time step T_s (with $s = 1, 2, ...Y$) may produce the opening/closing of each of the n-cracks acting along the beam. There will be a set of time intervals Δ_{t_j}, which begin at the time instant t_j during which the open cracks distribution is unchanged. The cracks distribution associated with a particular time interval is then described by a vector $\mathbf{\Lambda}_{\Delta_{t_j}} = \mathbf{\Lambda}(t_j)$. Once a change in cracks distribution is observed a new vector $\mathbf{\Lambda}_{\Delta_{t_j+1}}$ is computed.

As an example, in Fig. 1 the variation of cracks distribution of a beam with three switching cracks is shown. Initially all the cracks are closed. In this case, the time window is subdivided into 25 constant subintervals ΔT, so that $Y = 25$. Three transition instants and therefore three time intervals with fixed cracks distribution were obtained $\mathbf{\Lambda}_{\Delta_{t_0}}$, $\mathbf{\Lambda}_{\Delta_{t_1}}$ and $\mathbf{\Lambda}_{\Delta_{t_2}}$. The first transition instant, t_0, corresponds to the undamaged case. While t_1 and t_2 are characterised by 1 open crack and 2 open cracks, respectively.

Since during each Δ_{t_j} the crack distribution remains unchanged, the problem can be considered as a sequence of linear transient analysis, each of which is characterised by a specific open cracks distribution. As a result, in order to obtain the transient response over the entire time range, care must be taken in i) estimating the cracks distribution at each time step T_s by using Eq. (35); ii) identifying the transition instants; iii) enforcing continuity conditions between consequent linear transient analysis. These last two steps

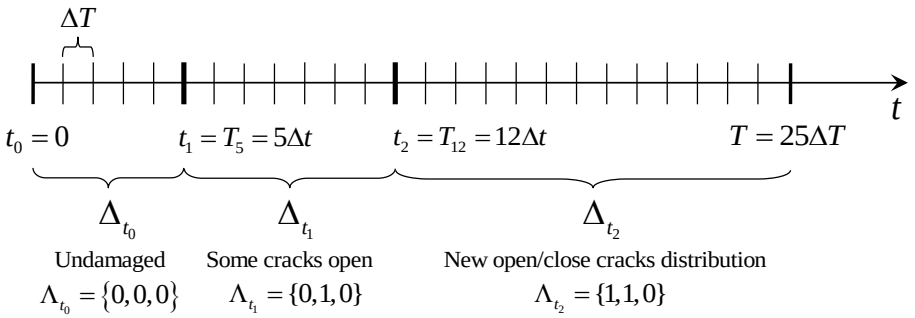

Figure 1: Example of variation of cracks distribution of a beam with three switching cracks over time.

are discussed in what follows.

4.2.1. Transition instants

The time interval with fixed open cracks distribution Δ_{t_0} finishes at an instant t_1, or in general the Δ_{t_j} finishes at an instant T_{s-1}, when at T_s:

$$\mathbf{\Lambda}_{\Delta_{t_j}} - \mathbf{\Lambda}_{T_s} \neq \mathbf{0}. \tag{57}$$

Then $T_s = t_{j+1}$, and t_{j+1} is called the "transition instant". When the transition instant occurs, the current linear analysis has to be stopped, and a new transient analysis with $\mathbf{\Lambda}_{\Delta_{t_{j+1}}} = \mathbf{\Lambda}(t_{j+1})$ has to be considered. However, this new analysis requires continuity conditions to be enforced, whose derivation is discussed in what follows.

4.2.2. Continuity conditions between linear transient analysis

At each transition instant t_j two continuity conditions have to be enforced in terms of displacement and velocity response with the cracks distribution

before t_k (i.e. $\mathbf{\Lambda}_{\Delta_{t_k}}$) and at transition instant t_k (i.e. $\mathbf{\Lambda}_{\Delta_{t_{k+1}}}$):

$$u(z, t_k, \mathbf{\Lambda}_{\Delta_{t_k}}) = u(z, t_k, \mathbf{\Lambda}_{\Delta_{t_{k+1}}}) \tag{58}$$

$$\dot{u}(z, t_k, \mathbf{\Lambda}_{\Delta_{t_k}}) = \dot{u}(z, t_k, \mathbf{\Lambda}_{\Delta_{t_{k+1}}}) \tag{59}$$

These continuity conditions can be used to evaluate the initial condition for a new linear analysis with fixed cracks distribution. As proposed by Caddemi et al. [13] for the analysis of a damaged beam under a moving load, the initial conditions can be obtained by using the orthogonality condition and by assuming that during the opening/closing of the cracks there is no dissipation of energy. In particular, they can be expressed as:

$$q_r(t_k) = \frac{\int_0^l u(z, t_k, \mathbf{\Lambda}_{\Delta_{t_k}}) \phi_r(z, \mathbf{\Lambda}_{\Delta_{t_{k+1}}}) \mathrm{d}z}{M_r^+} \tag{60}$$

$$\dot{q}_r(t_k) = \frac{\int_0^l \dot{u}(z\, t_k, \mathbf{\Lambda}_{\Delta_{t_k}}) \phi_r(z, \mathbf{\Lambda}_{\Delta_{t_{k+1}}}) \mathrm{d}z}{M_r^+} \tag{61}$$

where M_r^+ is the modal mass computed via Eq. (10) by using mode shapes of the beam for $\mathbf{\Lambda}_{\Delta_{t_{k+1}}}$. However, since a modal truncation is performed and there is a change in mode shape basis at the transition instant, the continuity conditions can be satisfied only in an approximate way. Caddemi et al. suggested a strategy based on energy arguments to quantify and verify that the error associated to the energy loss due to the modal basis variation is within a certain tolerance [13].

4.2.3. Computational strategy

To summarise, the transient analysis of damaged slender beams with switching cracks subject to moving masses requires the following steps:

1. At $t_0 = 0$ all the cracks can be assumed to be closed . Alternatively, an initial crack distribution can be assigned $\mathbf{\Lambda}(t_0)$.
2. The time interval Δ_{t_0} characterised by $\mathbf{\Lambda}_{\Delta_{t_0}} = \mathbf{\Lambda}(t_0)$ is identified. If the undamaged crack distribution is considered so that $\mathbf{\Lambda}_{\Delta_{t_0}} = \mathbf{0}$, the mode shapes and the corresponding natural frequencies of the undamaged beam are computed via Eq. (49). The response of the undamaged beam subject to moving masses is then calculated by using Eq. (5), having solved Eq. (55). Alternatively, the mode shapes and corresponding natural frequencies are calculated by using Eq. (45) with $\mathbf{\Lambda}_{\Delta_{t_0}} \neq \mathbf{0}$.
3. The strain $\widetilde{\epsilon}_j(T_s)$ at the centre of the jth crack is computed by using Eq. (34) and the Boolean variable $\lambda_j(T_s)$ is determined via Eq. (35) for each time step T_s of the analysis (starting from t_0). Such values are listed in the array $\mathbf{\Lambda}_{T_s}$ which specifies the open/closed status of the n cracks.
4. The first transition instant t_1 occurs when, $\mathbf{\Lambda}_{t_0} \neq \mathbf{\Lambda}_{T_s}$ and the transient linear analysis has to be stopped.
5. A new mode shape basis is calculated using Eq. (45) with $\mathbf{\Lambda}_{\Delta_{t_1}}$, and the continuity conditions (Eq. (61)) at the transition instant t_1 are enforced to produce a new set of initial conditions for the second linear analysis.
6. The second linear analysis with fixed mode shape basis with $\mathbf{\Lambda}_{\Delta_{t_1}}$ is performed in the interval Δ_{t_1}. The response of the damaged beam subject to moving masses is calculated via Eq. (5), solving Eq. (55) and using the mode shapes given by Eq. (45).
7. The strain $\widetilde{\epsilon}_j(T_s)$ at the centre of the jth crack is computed by using Eq. (34) and the Boolean variable $\lambda_j(T_s)$ is determined via Eq. (35) for

each time step T_s of the analysis (starting from t_1).

8. t_2 occurs when $\mathbf{\Lambda}_{\Delta_{t_1}} \neq \mathbf{\Lambda}_{T_s}$.
9. A new transient analysis has to be performed by considering the new mode shape basis with $\mathbf{\Lambda}_{\Delta_{t_2}}$ and new initial conditions.
10. Steps 7, 8 and 9 are repeated until the last moving mass reaches the end point of the damaged beam.

5. Numerical applications

Three numerical examples are presented in this section. In the first application, (Subsection 5.1), a simply-supported slender beam with one crack subject to a moving mass with constant velocity is investigated. Undamaged, always open crack and switching crack models are considered and compared. Moreover, the effect of the side, bottom or top, where the crack is located is also assessed. In addition to this, the case of two moving masses acting on the damaged beam is also investigated. The simply supported boundary condition is an idealisation of the boundary conditions of a bridge. In order to account for more complicated and realistic boundary conditions, the damaged Euler-Bernoulli beam with switching crack investigated in the first example is equipped with elastic constraints in the second numerical study (Subsection 5.2). The third numerical application is focused on the analysis of a multi-cracked beam. In particular, a clamped-clamped beam with two switching cracks under a moving mass is analysed.

In the forthcoming analysis, without loss of generality, the rotational stiffness K_j value employed for a given depth of the jth crack has been obtained by using the expression suggested by Bilello [19] valid for rectangular cross

sections:

$$K_j = \frac{EI_0}{h} \frac{0.9\left[(d_j/h) - 1\right]^2}{(d_j/h)\left[2 - (d_j/h)\right]}, \tag{62}$$

where h and d_j are the depths of the beam and of the jth crack, respectively.

5.1. Simply-supported beam with one crack under moving masses

In the first example, a simply supported damaged beam with parameters corresponding to those given by [6] is investigated. In particular, the beam has a square cross section of sides $h = 20$ cm, length $L = 20$ m, Young's modulus $E = 206$ GPa and density $\rho = 7,800$ kg/m^3 is considered. A crack with depth $d_1 = 15$ cm at the abscissa $\bar{z}_1 = l/2 = 10$ m has been considered. Eq. (62) yield the equivalent stiffness coefficients $K_1 = 8240$ kN m, to which correspond the dimensionless damage parameter (calculated via Eq. (31)) $\alpha_1 = 0.167$.

In the following subsections the influence of the side of the beam (upper or lower) where the crack is located on the beam response is investigated. Subsequently the case of two moving masses acting on the damaged beam is considered.

5.1.1. Single moving mass

The case under investigation is schematically depicted in Fig. 2. The beam is subjected to a moving mass $m = 1,000$ kg with constant velocity 5 m/s [6] starting from the left extreme of the beam. Three analyses have been carried out in total: (i) undamaged beam, (ii) beam with always open crack, and (iii) beam with switching crack.

The results are expressed in terms of the ratio of the dynamic deflection at the midpoint to the static deflection due to the mass acting at the midpoint,

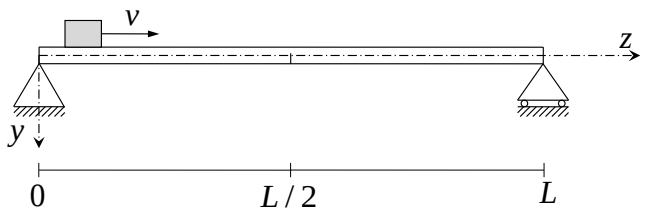

Figure 2: Damaged simply supported beam subject to a moving mass

$u/u_{static,max}$, versus the normalised position of the moving mass, vt/L. The static deflection at the midpoint of simply supported beam loaded by the weight of the mass is given by $(\rho A_0 L^3)/(48EI_0)$, where A_0 is the undamaged cross-sectional area and EI_0 is the reference value of the flexural stiffness with I being the second moment of area.

For the undamaged case, the first four natural frequencies of the beam are computed with Eq. (49): $\Omega_{\text{und}} = [7.32, 29.28, 65.89, 117.135]\,\text{rad/s}$. These natural frequencies and the corresponding mode shapes have been validated by building a Finite Element (FE) model of the beam with SAP2000 [20]. The response of the undamaged beam subject to the moving mass is then calculated by using Eq. (5), having solved Eq. (16). The results obtained are in perfect agreement with those obtained in reference [6]; In Figure 3, the Newmark integration method results are compared to the transition matrix results showing a perfect agreement. For each analysis, the time variable has been subdivided in 700 time intervals, each of duration 0.0057s.

When the crack is open and described by the flexibility model of cracks, Eq. (49) yields $\Omega_{\text{AOC}} = [6.34, 29.28, 58.71, 117.135]\,\text{rad/s}$. These results and the corresponding modes have been validated by building a FE model of the

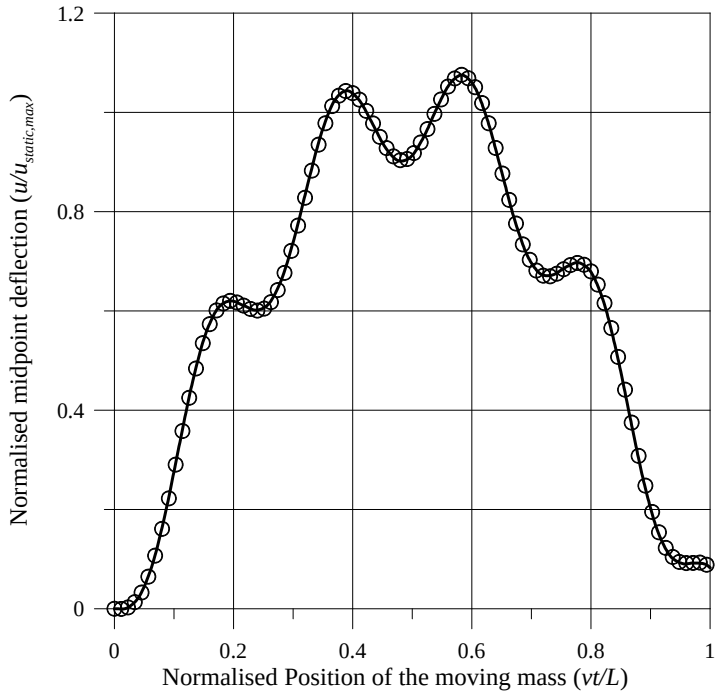

Figure 3: Dimensionless transverse deflection, $u/u_{static,max}$, versus the normalised position of the moving mass, vt/l - undamaged case. Solid line: transition matrix results; circle marker: Newmark integration results

beam with an open cracks (by applying a release partial fixity at the crack' location in SAP2000). It is worth noting that only the first and third natural frequencies are affected by the crack. As a matter of fact, the second and fourth mode shapes have a nodal point at the centre of the beam, where the crack is located, so they remain unchanged. Knowing the mode shapes, the response of the damaged beam subject to the moving mass is calculated by using Eq. (5), having solved Eq. (16). The solution obtained with the proposed approach (by using the transition matrix) are validated by applying the Newmark integration method in Figure 4, showing a very good agreement.

In the same figure, the results obtained for the always open crack are compared to the undamaged results. It is possible to observe that the presence of a single always open crack produces larger amplitude vibrations. In particular, the maximum dimensionless deflection has increased from 1.075 (undamaged) to 1.603 (always open crack).

The crack is now assumed to be closed at t_0 and verified if open/close status at each time step of the analysis. Moreover, both top and bottom location are considered . Following the procedure described in Section 4, it has been found that there are two transition instants, which are indicated as t_1 (crack open) and t_2 (crack closed) in Figure 5. Moreover, it can be observed that the results obtained (thick dash-dot-dot grey line) coincide with the thick solid black line (undamaged case).

It can be noticed that, for the case under investigation, employing the always open crack model would largely overestimate the normalised transversal vibration.

Now let us consider the case in which the switching crack is located on

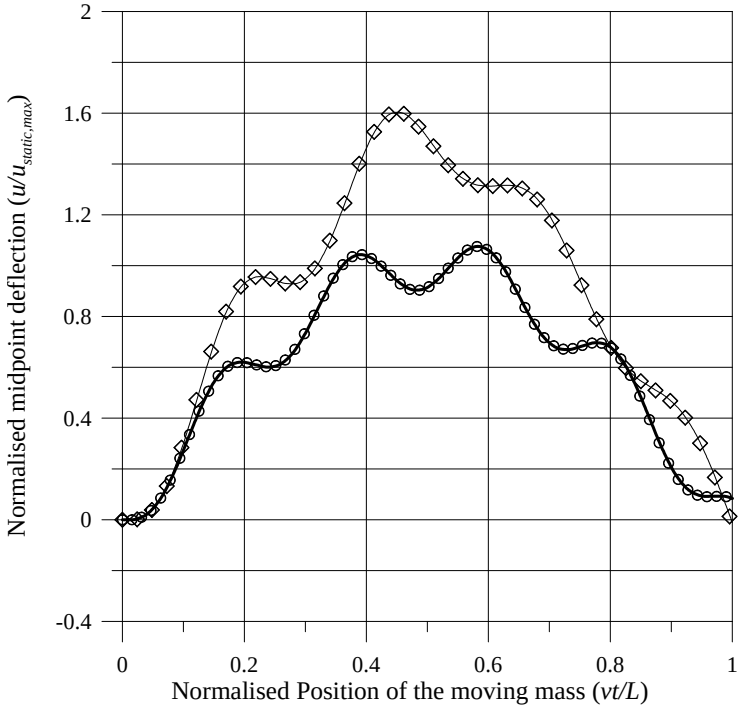

Figure 4: Dimensionless transverse deflection, $u/u_{static,max}$, versus the normalised position of the moving mass, vt/L - undamaged case (thick solid line) versus always open crack (thin solid line). Circle and diamond markers: Newmark integration results

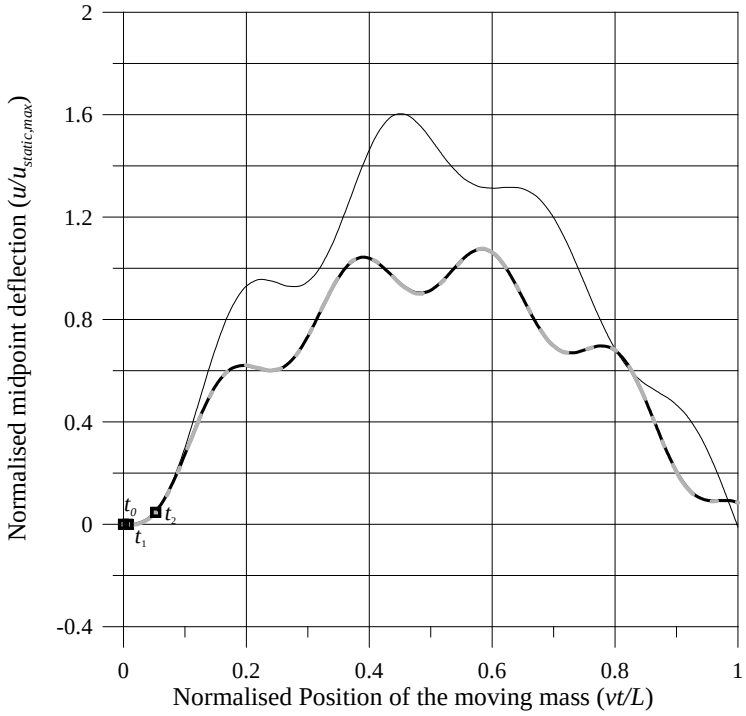

Figure 5: Dimensionless transverse deflection, $u/u_{static,max}$, versus the normalised position of the moving mass, vt/L - comparison of undamaged case (thick solid black line), always open crack (thin solid black line) and switching crack on the bottom side of the beam (thick dash-dot-dot grey line). t_0 is the initial instant and t_1 and t_2 are the transition instants.

the upper side of the beam. The results obtained for this configuration are shown in Figure 6. The transition instants are again two, but they occur at different time steps. As a result, the crack is open for a longer time interval leading to a dimensionless transverse deflection (thick dash-dot-dot grey line) conforming with that obtained with the always open crack model (thin solid black line).

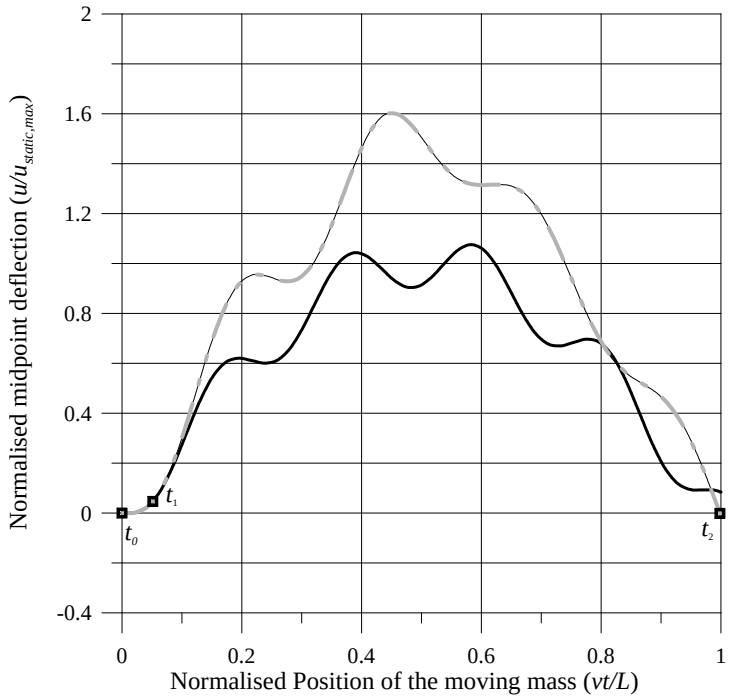

Figure 6: Dimensionless transverse deflection, $u/u_{static,max}$, versus the normalised position of the moving mass, vt/L - comparison of undamaged case (thick solid black line), always open crack (thin solid black line) and switching crack on the top side of the beam (thick dash-dot-dot grey line). t_0 is the initial instant and t_1 and t_2 are the transition instants.

It can be concluded that for the simply supported damaged beam under investigation: (i) the crack produces large deflections, (ii) the side where the

crack is located significantly affects the response; and (iii) the open crack and undamaged solutions provide, respectively, the upper and lower bounds of the transversal vibration.

5.1.2. Two moving masses

Let us now consider two moving masses acting on the same beam. While the first moving mass has the same properties of that studied in the previous case (i.e. $m_1 = 1,000$ kg and $v_1 = 5$ m/s), the second moving mass is characterised by: $m_1 = 1,000$ kg and $v_1 = 10$ m/s and at the beginning of the analysis (i.e. at t_0) is located at $7L/10$. The problem under investigation is schematically described in Fig. 7.

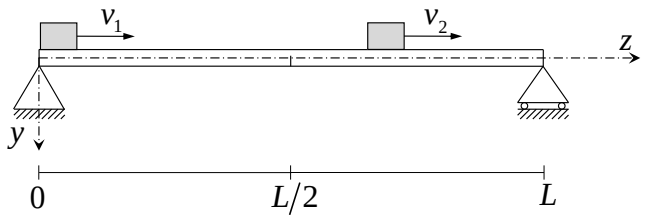

Figure 7: Damaged simply supported beam subject to two moving masses shown at t_0

For this analysis the first six natural frequencies of the beam were considered. The response is expressed in terms of the ratio of the dynamic deflection at the midpoint to the static deflection due to the first mass only acting at the midpoint, $u/u_{static,max1}$, versus the normalised position of the first moving mass, $v_1 t/L$.

The always open crack and undamaged results are shown in Figure 8 and they have been validated with the Newmark integration scheme. The second moving mass has produced larger normalised transversal displacements in

both configurations. The larger response is again obtained for the always open crack configuration.

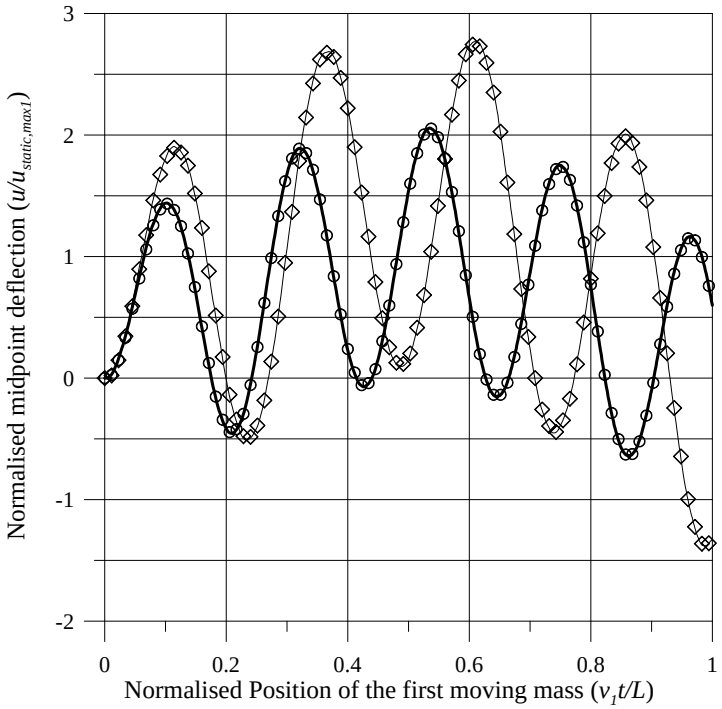

Figure 8: Dimensionless transverse deflection, $u/u_{static,max1}$, versus the normalised position of the first moving mass, $v_1 t/L$ - undamaged case (thick solid line) versus always open crack case (thin solid line). Circle and diamond markers: Newmark integration results.

As for the previous case, the crack is now assumed to be located on the lower side of the beam and its switching behaviour is taken into account (starting from a closed crack configuration). In this case there are six transition instants: t_1, t_3 and t_5, at which the crack opens, while it closes at t_2, t_4 and t_6. The result obtained are compared with the undamaged and always open results in Figure 9. In this case it is possible to observe that the re-

sponse would be coincident with the undamaged case until the transition instant t_3, after which it is possible to observe some small deviations.

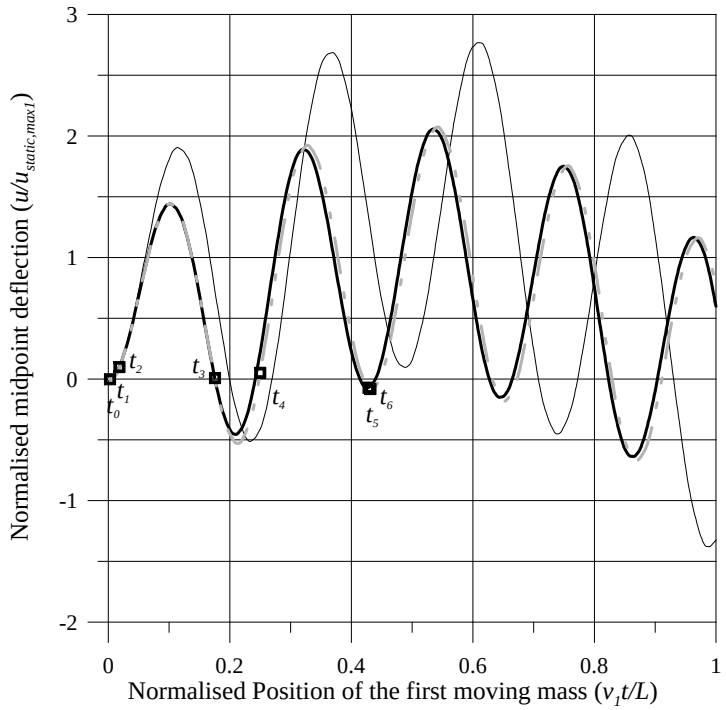

Figure 9: Dimensionless transverse deflection, $u/u_{static,max1}$, versus the normalised position of the moving mass, $v_1 t/L$ - comparison of undamaged case (thick line), damage case (thin line) and switching crack at the bottom side of the beam (thick dash-dot-dot grey line). t_0 is the initial instant. t_1, t_3 and t_5 are the transition instants at which crack opens, while it closes at t_2, t_4 and t_6.

If a switching crack is now considered on the top side of the beam, the dimensionless response corresponds to the one depicted in Figure 10. Again, six transition instants can be identified: t_1, t_3 and t_5, at which the crack opens, while it closes at t_2, t_4 and t_6. The response conforms to the open

crack response until the transition instant t_2, after which it is possible to observe some small deviations which increase after t_5.

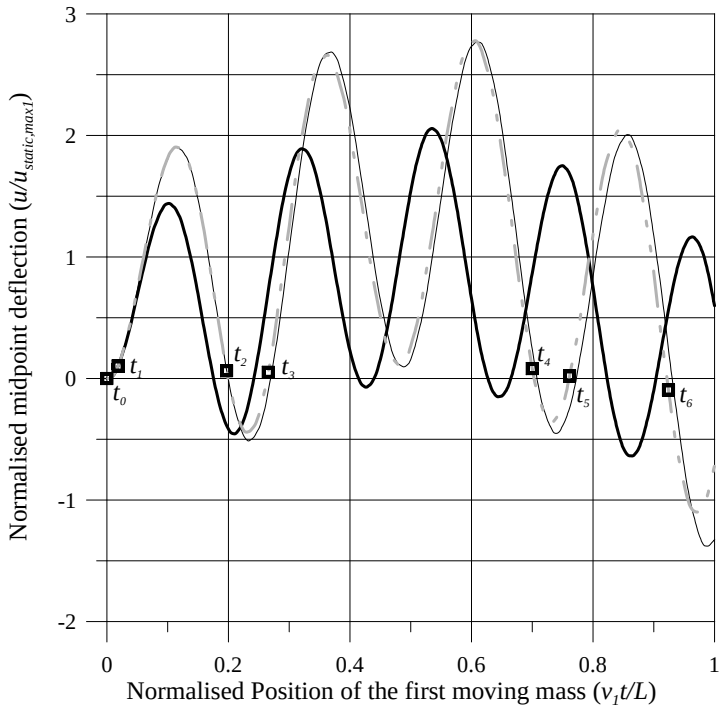

Figure 10: Dimensionless transverse deflection, $u/u_{static,max1}$, versus the normalised position of the moving mass, $v_1 t/L$ - comparison of undamaged case (thick line), damage case (thin line) and switching crack at the top side of the beam (thick dash-dot-dot grey line). t_0 is the initial instant where the crack is closed. t_1, t_3 and t_5 are the transition instants at which crack opens, while it closes at t_2, t_4 and t_6.

From the above results, it is possible to conclude that the always open crack and undamaged cases cannot be considered as bounding responses for the switching crack cases when two moving masses are acting on the same simply supported beam with one crack which was considered in the previous numerical example. Therefore, if multiple moving masses are applied to a

simply supported beam with one centred switching crack, using the always open and undamged models as limiting conditions might not provide bounds to the switching crack response.

5.2. Damaged beam with elastic constraints subject to a moving mass

In the second numerical example, the damaged beam with elastic boundary conditions depicted in Figure 11 with left-end rotational spring support, and right-end rotational and translational springs support constraints, is investigated.

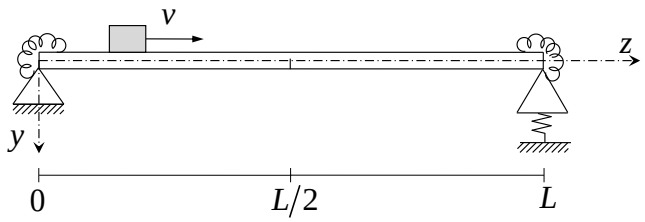

Figure 11: Damaged beam with flexible boundary conditions subject to a moving mass

The properties of the beam, moving mass and the damage condition correspond to those assumed in the first example. The boundary conditions are now such that the left-end rotational spring is $k_{r,L} = 10^7$Nm, and right-end rotational and translational springs are $k_{r,R} = 10^4$Nm and $k_{t,R} = 10^6$N/m, respectively.

The natural frequencies of the undamaged beam are obtained by using Eq. (49): $\Omega_{\text{und}} = [10.04, 36.01, 78.05, 134.3, 204.7, 289.43, 388.63, 502.37]$ rad/s. While the natural frequencies obtained by considering the always open crack are: $\Omega_{\text{AOC}} = [8.93, 36.00, 69.7, 133.53, 187.68, 287.21, 361.778, 498.436]$ rad/s. By comparing the two natural frequencies vectors, it is possible to observe

that the second mode is the one least affected by the crack. These results and the corresponding modes have been validated by building a FE model of the undamaged beam and of the beam with an open cracks, respectively.

The results obtained considering the always-open crack model, the switching crack model (with the crack positioned on either side of the beam) and the undamaged case are compared in Figures 12 and 13, where the ratio of the dynamic deflection at the midpoint to the static deflection of the equivalent simply supported beam are plotted against the normalised position of the moving mass.

By comparing the results shown in Figures 12 and 13 with the corresponding ones obtained with the simply-supported constraints (Figures 5 and 6, respectively), it is possible to observe a significant change in the response signature, in terms of amplitude and shape, due to the flexible constraints. Moreover, as observed for the simply supported damaged beam subject to a moving mass, the always open crack and undamaged models provide bounds on the transversal displacement obtained when considering the switching crack behaviour.

5.3. Multi-damaged beam with clamped-clamped boundary conditions subject to a moving mass

In the third numerical example, the multi-damaged beam with fixed boundary conditions shown in Figure 14 has been investigated.

The beam has a rectangular cross section with width $b = 45$cm and depth $h = 30$ cm, length $L = 30$m, Young's modulus $E = 200$ GPa and density $\rho = 7,900$ kg/m^3. Two equally-spaced cracks with depths $d_1 = d_2 = 20$ cm at the abscissas $\bar{z}_1 = L/3 = 10$ m and $\bar{z}_1 = 2L/3 = 20$ m have been considered. The

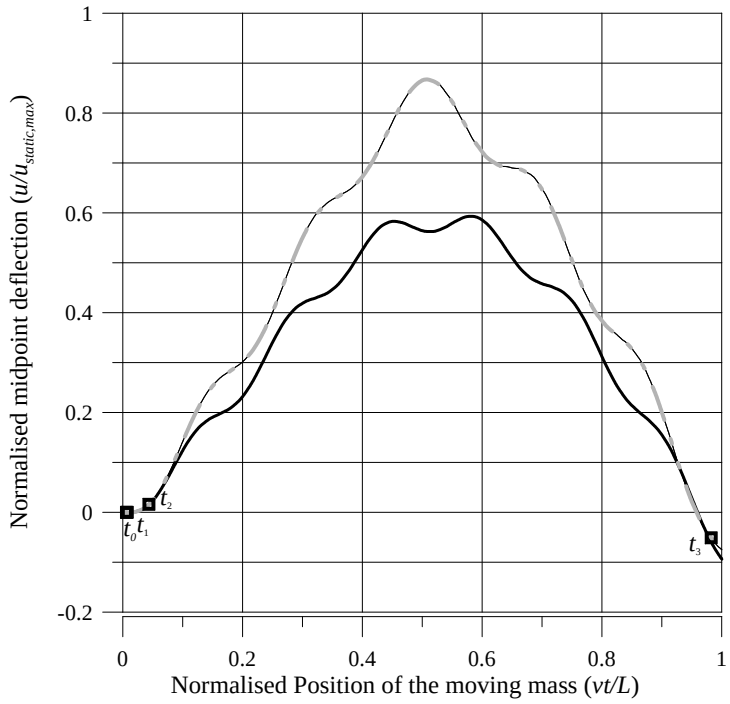

Figure 12: Flexible boundary condition results. Dimensionless transverse deflection, $u/u_{static,max}$, versus the normalised position of the moving mass, vt/L - comparison of undamaged case (thick solid line), open crack (thin solid line) and switching crack at the top side of the beam (thick dash-dot-dot grey line). t_0 is the initial instant where the crack is closed. t_1, t_2, t_3 and t_4 are the transition instants.

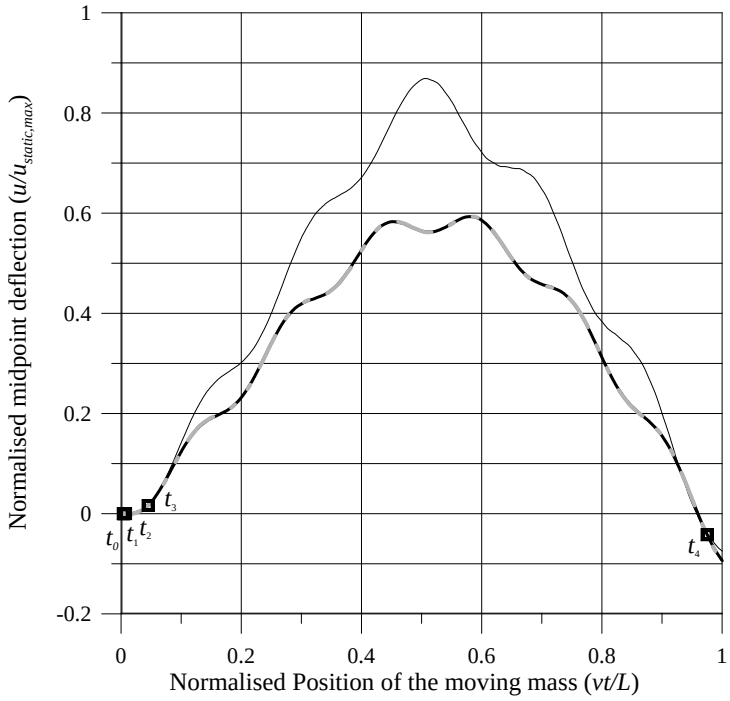

Figure 13: Flexible boundary condition results. Dimensionless transverse deflection, $u/u_{static,max}$, versus the normalised position of the moving mass, vt/L - comparison of undamaged case (thick solid line), damage case (thin solid line) and switching crack at the bottom side of the beam (thick dash-dot-dot grey line). t_0 is the initial instant where the crack is closed. t_1, t_2 and t_3 are the transition instants.

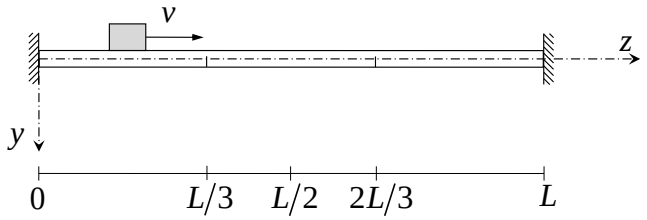

Figure 14: Clamped-clamped beam with two equally spaced damages subject to a moving mass

elastic stiffness of the equivalent discrete springs are $K_1 = K_1 = 7594$ kN m, to which correspond the dimensionless damage parameters (calculated via Eq. (62)) $\alpha_1 = \alpha_2 = 0.089$. The beam is subjected to a moving mass $m = 3,000$ kg with constant velocity 20 m/s starting from the left extreme of the beam.

The natural frequencies obtained for various open cracks configurations are listed in Table 1.

Table 1: Natural frequencies (rad/s) of the clamped-clamped beam with switching cracks

Mode Number	Undamaged	First crack open	Second crack open	both cracks open
	$\mathbf{\Lambda} = \{0, 0\}$	$\mathbf{\Lambda} = \{1, 0\}$	$\mathbf{\Lambda} = \{0, 1\}$	$\mathbf{\Lambda} = \{1, 1\}$
1	10.83	10.60	10.60	10.41
2	29.86	28.09	28.09	26.31
3	58.54	58.30	58.30	58.04
4	96.76	93.29	93.29	90.88
5	144.55	136.74	136.74	128.14
6	201.89	201.11	201.11	200.15
7	268.79	260.49	260.49	255.53
8	345.25	329.61	329.61	311.18
9	431.22	429.84	429.84	428.00

From Table 1, it can be observed that all the natural frequencies reduce when the cracks are open. Moreover, given the symmetry of the system, the natural frequencies obtained when only one of the cracks is open, i.e.

$\mathbf{\Lambda} = \{0, 1\}$ and $\mathbf{\Lambda} = \{1, 0\}$, are exactly the same. However, the corresponding mode shapes would be different because they will display a discontinuity at the crack location. Therefore, they'll lead to a different transverse vibration response.

Four cases of switching cracks have been investigated such that the cracks where located on the same side, i.e. (low, low) and (top,top), or on opposite sides, i.e. (top, low) and (low, top). For each case the switching crack model is compared with the results yielded by (i) the undamaged model; (ii) always open crack model; (iii) closed-open model and (iv) open-closed model.

The vibration response of the clamped-clamped beam with switching cracks located at the bottom side of the beam is shown in Figure 15. For this case 6 transition instants were identified with cracks distribution summarised in Table 2. As shown in Figure 15, the response obtained (thick dash-dot-dot grey line) is following that obtained with the undamaged model (thick solid black line).

When the first switching crack is located on the bottom side and the second one is located at the top side of the beam, 5 transition instants were identified (whose cracks distribution is summarised in the third column of Table 2). As shown in Figure 16, the response obtained (thick dash-dot-dot grey line) is following that obtained with the closed-open crack model (thick dashed black line).

In Figure 17, the response obtained by considering the first switching crack on the top side and the second at the bottom side of the beam is shown. In this case 16 transition instants were identified (whose cracks distribution is summarised in the forth column of Table 2). In this case, the response

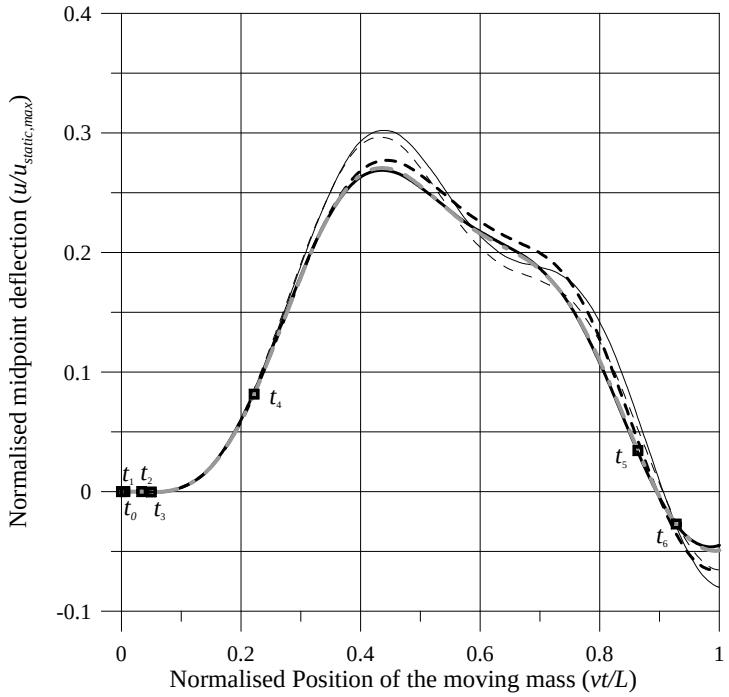

Figure 15: Results of the clamped-clamped beam with cracks on the bottom. Dimensionless transverse deflection, $u/u_{static,max}$, versus the normalised position of the moving mass, vt/l. Thick solid black line: undamaged beam; Thin solid black line: always open crack; Thin dashed black line: open-closed. Thick dashed black line: closed-open. Thick dash-dot-dot grey line: switching crack. t_0 is the initial instant where the crack is closed. t_1 to t_6 are the transition instants.

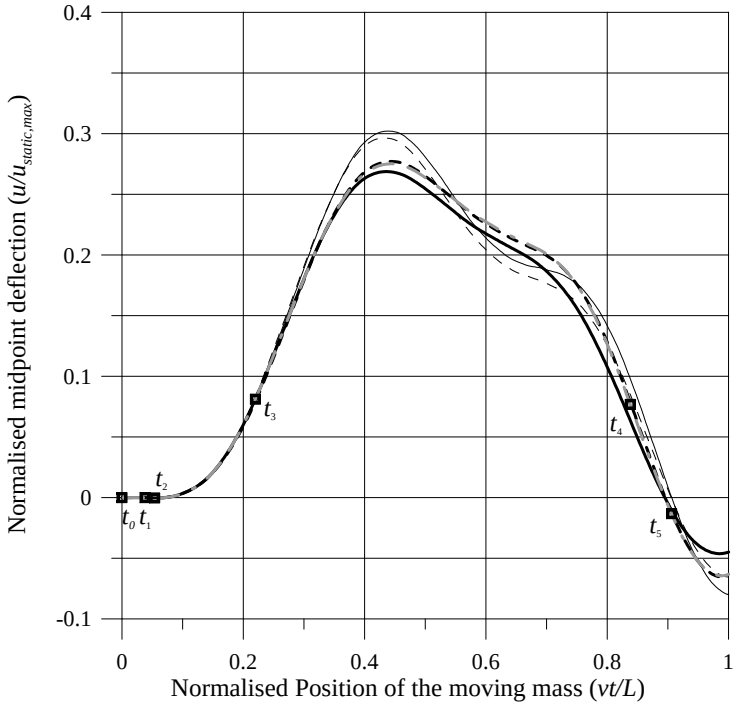

Figure 16: Results of the clamped-clamped beam with cracks on the low and top side of the beam, respectively. Dimensionless transverse deflection, $u/u_{static,max}$, versus the normalised position of the moving mass, vt/l. Thick solid black line: undamaged beam; Thin solid black line: always open crack; Thin dashed black line: open-closed. Thick dashed black line: closed-open. Thick dash-dot-dot grey line: switching crack. t_0 is the initial instant where the crack is closed. t_1 to t_5 are the transition instants.

obtained (thick dash-dot-dot grey line) is following that obtained with the open-closed crack model (thin dashed black line).

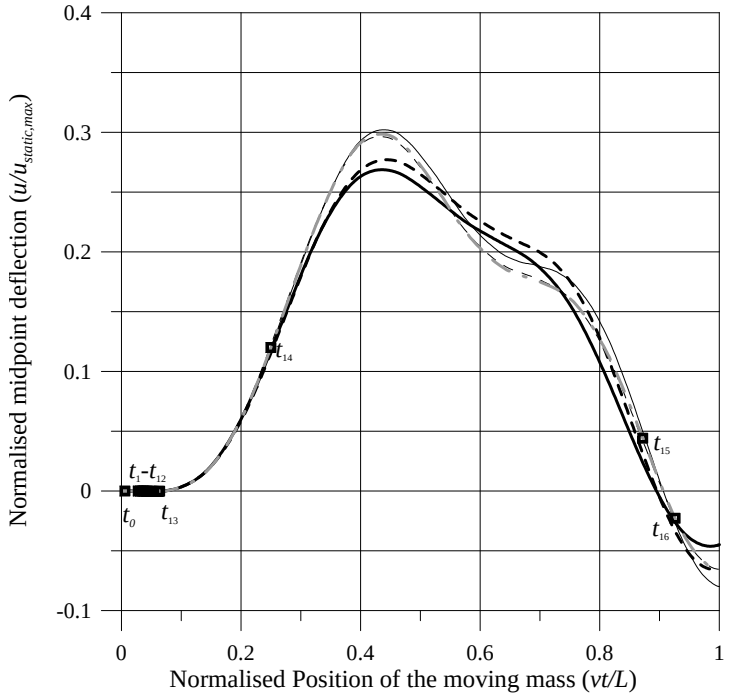

Figure 17: Results of the clamped-clamped beam with cracks on the top and low side of the beam, respectively. Dimensionless transverse deflection, $u/u_{static,max}$, versus the normalised position of the moving mass, vt/l. Thick solid black line: undamaged beam; Thin solid black line: always open crack; Thin dashed black line: open-closed. Thick dashed black line: closed-open. Thick dash-dot-dot grey line: switching crack. t_0 is the initial instant where the crack is closed. t_1 to t_{16} are the transition instants.

Finally, the case in which the two switching cracks are both located on the top side of the beam is considered. 10 transition instants were identified (whose cracks distribution is summarised in the last column of Table 2). From Figure 18, it is possible to observe that the response obtained (thick

dash-dot-dot grey line) is following that obtained with the always crack model (thin solid line).

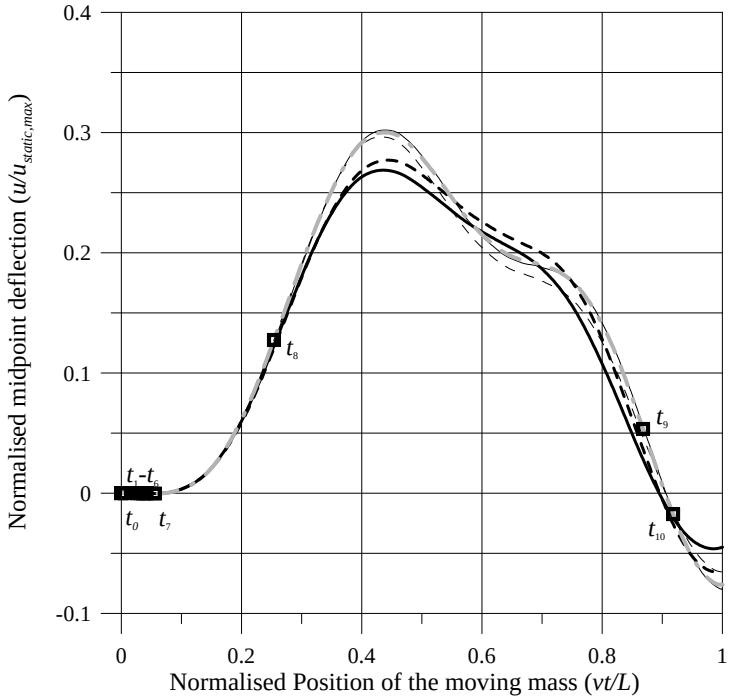

Figure 18: Results of the clamped-clamped beam with cracks on the top side of the beam. Dimensionless transverse deflection, $u/u_{static,max}$, versus the normalised position of the moving mass, vt/l. Thick solid black line: undamaged beam; Thin solid black line: always open crack; Thin dashed black line: open-closed. Thick dashed black line: closed, open. Thick dash-dot-dot grey line: switching crack. t_0 is the initial instant where the crack is closed. t_1 to t_{10} are the transition instants.

From the above results it can be concluded that for the clamped-clamped beam with two switching cracks subject to a moving mass, the bounds on the response can be obtained by performing four analyses with fixed cracks distribution and considering the envelope of these results .

Table 2: Cracks status (open=1; closed=0) at each transition instant for the clamped-clamped beam with switching cracks assigned either at the top or at the bottom side of the beam.

Transition instant	$\{\text{low}, \text{low}\}$ (see Fig. 15)	$\{\text{low}, \text{top}\}$ (see Fig. 16)	$\{\text{top}, \text{low}\}$ (see Fig. 17)	$\{\text{top}, \text{top}\}$ (see Fig. 18)
t_0	$\{0,0\}$	$\{0,0\}$	$\{0,0\}$	$\{0,0\}$
t_1	$\{0,1\}$	$\{0,1\}$	$\{1,1\}$	$\{1,0\}$
t_2	$\{0,0\}$	$\{0,0\}$	$\{0,1\}$	$\{0,0\}$
t_3	$\{0,1\}$	$\{0,1\}$	$\{1,1\}$	$\{1,0\}$
t_4	$\{0,0\}$	$\{1,1\}$	$\{1,0\}$	$\{1,1\}$
t_5	$\{1,0\}$	$\{1,0\}$	$\{0,0\}$	$\{0,1\}$
t_6	$\{1,1\}$	-	$\{1,0\}$	$\{1,1\}$
t_7	-	-	$\{1,1\}$	$\{1,0\}$
t_8	-	-	$\{1,0\}$	$\{1,1\}$
t_9	-	-	$\{0,0\}$	$\{0,1\}$
t_{10}	-	-	$\{1,0\}$	$\{0,0\}$
t_{11}	-	-	$\{1,1\}$	-
t_{12}	-	-	$\{1,0\}$	-
t_{13}	-	-	$\{1,1\}$	-
t_{14}	-	-	$\{1,0\}$	-
t_{15}	-	-	$\{0,0\}$	-
t_{16}	-	-	$\{0,1\}$	-

6. Concluding remarks

In this paper the dynamic analysis of Euler-Bernoulli beams with switching cracks subjected to moving masses has been investigated. Some common macro-scale assumptions on the behaviour of cracks have been made: *i*) cracks can be modelled through equivalent internal springs (with a linear moment-rotation constitutive law, when open); and *ii*) degradation effects are negligible. The "flexibility model of switching cracks" has been extended to account for the fact that the induced deformed shape at each instant might vary, resulting in a time-dependent open-cracks distribution. In particular, each crack can be either open or closed (no breathing crack behaviour is considered), depending on the sign of elastic axial strain calculated at the crack centre at each time step.

By using the flexibility model of cracks, it was possible to evaluate the closed-form solution of the mode shapes of a beam with any number of assigned always open cracks. This result enabled the evaluation of the transient solution by employing the mode-superposition method. Moreover, an efficient numerical integration scheme based on transition matrix strategy has been applied and validated to solve the governing equations of a beam with always open cracks subject to moving masses.

A simple yet effective computational strategy was devised to include the switching crack behaviour. This strategy is based on checking the open cracks distribution at each time step of the analysis, and identifying the so-called 'transition instants'. This procedure requires enforcing continuity conditions at each transition instant in order to account for the change in the mode shape basis.

Three types of numerical applications were investigated, showing the versatility of the proposed approach in tackling multiple moving masses and flexible boundary conditions problems under switching cracks. . The numerical applications have shown that (i) the always-open crack assumption, widely adopted for many engineering applications, may overestimate or underestimate the transverse response of a beam with switching cracks under moving masses. Therefore, it cannot be used as an upper bound on the results yielded by the switching cracks model under multiple moving masses; (ii) including elastic constraints can yield significantly different results compared to the widely adopted simply-supported beam model under a moving mass; (iii) the side where the crack is located can largely affect the response of the damaged beam under moving masses; (iv) the response of a beam with switching cracks under moving masses is not always bounded by the always-open crack model and by the undamaged case: this can be caused by the effect of multiple masses or by the presence of multiple cracks.

7. Acknowledgements

AC is grateful to Balliol College for the Career Development Fellowship in Engineering, and to Dr Alessandro Cabboi for providing feedback on an initial version of this manuscript. AC would also like to thank the anonymous reviewers for their constructive comments.

References

[1] L. Fryba, Vibration of Solids and Structures under Moving Loads, Noordhoff, Groningen, 1972.

[2] H. Ouyang, Moving-load dynamic problems: A tutorial (with a brief overview), Mechanical Systems and Signal Processing 25 (6) (2011) 2039 – 2060. doi:10.1016/j.ymssp.2010.12.010.

[3] M. I. Friswell, J. E. T. Penny, Crack modeling for structural health monitoring, Structural Health Monitoring 1 (2002) 139–148.

[4] A. Dimarogonas, Vibration of cracked structures: a state of the art review, Engineering Fracture Mechanics 55 (1996) 831–857.

[5] C. Bilello, L. Bergman, Vibration of damaged beams under a moving mass: theory and experimental validation, Journal of Sound and Vibration 274 (3?5) (2004) 567 – 582. doi:10.1016/j.jsv.2003.01.001.

[6] Y. Pala, M. Reis, Dynamic response of a cracked beam under a moving mass load, Journal of Engineering Mechanics 139 (9) (2013) 1229–1238. doi:10.1061/(ASCE)EM.1943-7889.0000558.

[7] T. Chondros, A. Dimarogonas, J. Yao, A continuous cracked beam vibration theory, Journal of Sound and Vibration 251 (1998) 17–34.

[8] A. Ariaei, S. Ziaei-Rad, M. Ghayour, Vibration analysis of beams with open and breathing cracks subjected to moving masses, Journal of Sound and Vibration 326 (3?5) (2009) 709 – 724. doi:10.1016/j.jsv.2009.05.013.

[9] K. V. Nguyen, Comparison studies of open and breathing crack detections of a beam-like bridge subjected to a moving vehicle, Engineering Structures 51 (2013) 306 – 314. doi:http://dx.doi.org/10.1016/j.engstruct.2013.01.018.

[10] C. Fu, The effect of switching cracks on the vibration of a continuous beam bridge subjected to moving vehicles, Journal of Sound and Vibration 339 (0) (2014) 157–175. doi:10.1016/j.jsv.2014.11.009.

[11] A. Cicirello, A. Palmeri, Static analysis of Euler-Bernoulli beams with multiple unilateral cracks under combined axial and transverse loads, International Journal of Solids and Structures 51 (5) (2014) 1020 – 1029. doi:10.1016/j.ijsolstr.2013.11.030.

[12] M. Ahmadi, A. Nikkhoo, Utilization of characteristic polynomials in vibration analysis of non-uniform beams under a moving mass excitation, Applied Mathematical Modelling 38 (7) (2014) 2130 – 2140. doi:https://doi.org/10.1016/j.apm.2013.10.011.

[13] S. Caddemi, I. Calió, M. Marletta, The non-linear dynamic response of the Euler-Bernoulli beam with an arbitrary number of switching cracks, International Journal of Non-Linear Mechanics 45 (2010) 714–726.

[14] S. Caddemi, I. Calió, Exact closed-form solution for the vibration modes of the Euler-Bernoulli beam with multiple open cracks, Journal of Sound and Vibration 327 (2009) 473–489.

[15] V. D. Salvo, G. Muscolino, A. Palmeri, A substructure approach tailored to the dynamic analysis of multi-span continuous beams under moving loads, Journal of Sound and Vibration 329 (15) (2010) 3101 – 3120. doi:https://doi.org/10.1016/j.jsv.2010.02.016.

[16] A. Palmeri, A. Cicirello, Physically-based Diracs delta functions in the

static analysis of multi-cracked Euler-Bernoulli and Timoshenko beams, International Journal of Solids and Structures 48 (2011) 2184–2195.

[17] W. L. Brogan, Modern Control Theory (3rd Ed.), Prentice-Hall, Inc., Upper Saddle River, NJ, USA, 1991.

[18] A. Nikkhoo, F. Rofooei, M. Shadnam, Dynamic behavior and modal control of beams under moving mass, Journal of Sound and Vibration 306 (2007) 712 – 724. doi:10.1016/j.jsv.2007.06.008.

[19] C. Bilello, Theoretical and experimental investigation on damaged beams under moving systems, PhD Thesis, Università degli Studi di Palermo (Italy), 2001.

[20] SAP2000, CSi: Computers and Structures, Inc., Version 14.1.0, computer software.

8. Appendix: Example of common boundary conditions

Example of common boundary conditions at 0 (or equivalently at 1) are:

- free: $\widetilde{\phi}''(0,\mathbf{\Lambda}) = 0$ and $\widetilde{\phi}'''(0,\mathbf{\Lambda}) = 0$;
- pinned: $\widetilde{\phi}(0,\mathbf{\Lambda}) = 0$ and $\widetilde{\phi}''(0,\mathbf{\Lambda}) = 0$;
- clamped: $\widetilde{\phi}(0,\mathbf{\Lambda}) = 0$ and $\widetilde{\phi}'(0,\mathbf{\Lambda}) = 0$.

Moreover, for flexible boundary conditions:

- rotational spring support with spring stiffness k_φ, in dimensionless form $\widetilde{k}_\varphi = (k_\varphi l)/(EI_0)$:

- at $\zeta = 0$: $\widetilde{\phi}(0, \mathbf{\Lambda}) = 0$ and $\widetilde{EI}(0)\, \widetilde{\phi}''(0, \mathbf{\Lambda}) = \widetilde{k}_{\varphi}\, \widetilde{\phi}'(0, \mathbf{\Lambda})$;
- at $\zeta = 1$: $\widetilde{\phi}(1, \mathbf{\Lambda}) = 0$ and $\widetilde{EI}(1)\, \widetilde{\phi}''(1, \mathbf{\Lambda}) = -\widetilde{k}_{\varphi}\, \widetilde{\phi}'(1, \mathbf{\Lambda})$

- translational spring support with spring stiffness k_t, in dimensionless form $\widetilde{k}_t = (k_t l^3)/(EI_0)$:
  - at $\zeta = 0$: $\widetilde{\phi}''(0, \mathbf{\Lambda}) = 0$ and $\widetilde{EI}(0)\, \widetilde{\phi}'''(0, \mathbf{\Lambda}) = \widetilde{k}_t\, \widetilde{\phi}(0, \mathbf{\Lambda})$;
  - at $\zeta = 1$: $\widetilde{\phi}''(1, \mathbf{\Lambda}) = 0$ and $\widetilde{EI}(1)\, \widetilde{\phi}'''(1, \mathbf{\Lambda}) = -\widetilde{k}_{\varphi}\, \widetilde{\phi}(1, \mathbf{\Lambda})$

List of Tables

Mode Number	Undamaged	First crack open	Second crack open	both cracks open
	$\mathbf{\Lambda} = \{0, 0\}$	$\mathbf{\Lambda} = \{1, 0\}$	$\mathbf{\Lambda} = \{0, 1\}$	$\mathbf{\Lambda} = \{1, 1\}$
1	10.83	10.60	10.60	10.41
2	29.86	28.09	28.09	26.31
3	58.54	58.30	58.30	58.04
4	96.76	93.29	93.29	90.88
5	144.55	136.74	136.74	128.14
6	201.89	201.11	201.11	200.15
7	268.79	260.49	260.49	255.53
8	345.25	329.61	329.61	311.18
9	431.22	429.84	429.84	428.00

Transition instant	$\{low, low\}$ (see Fig. 15)	$\{low, top\}$ (see Fig. 16)	$\{top, low\}$ (see Fig. 17)	$\{top, top\}$ (see Fig. 18)
t_0	$\{0, 0\}$	$\{0, 0\}$	$\{0, 0\}$	$\{0, 0\}$
t_1	$\{0, 1\}$	$\{0, 1\}$	$\{1, 1\}$	$\{1, 0\}$
t_2	$\{0, 0\}$	$\{0, 0\}$	$\{0, 1\}$	$\{0, 0\}$
t_3	$\{0, 1\}$	$\{0, 1\}$	$\{1, 1\}$	$\{1, 0\}$
t_4	$\{0, 0\}$	$\{1, 1\}$	$\{1, 0\}$	$\{1, 1\}$
t_5	$\{1, 0\}$	$\{1, 0\}$	$\{0, 0\}$	$\{0, 1\}$
t_6	$\{1, 1\}$	-	$\{1, 0\}$	$\{1, 1\}$
t_7	-	-	$\{1, 1\}$	$\{1, 0\}$
t_8	-	-	$\{1, 0\}$	$\{1, 1\}$
t_9	-	-	$\{0, 0\}$	$\{0, 1\}$
t_{10}	-	-	$\{1, 0\}$	$\{0, 0\}$
t_{11}	-	-	$\{1, 1\}$	-
t_{12}	-	-	$\{1, 0\}$	-
t_{13}	-	-	$\{1, 1\}$	-
t_{14}	-	-	$\{1, 0\}$	-
t_{15}	-	-	$\{0, 0\}$	-
t_{16}	-	-	$\{0, 1\}$	-

List of Figures